frontiers in Chemistry

REVIEW
published: 06 December 2021
doi: 10.3389/fchem.2021.786607

Research Progress of Gas Sensing Performance of 2D Hexagonal WO_3

Yueqi Li, Qin Zhou, Shoubing Ding and Zhimin Wu**

Chongqing Key Laboratory of Photoelectric Functional Materials, College of Physics and Electronic Engineering, Chongqing Normal University, Chongqing, China

Metal oxide semiconductor gas sensing materials have attracted great research interest in the gas sensor field due to their outstanding physical and chemical properties, low cost, and easy preparation. Among them, two-dimensional hexagonal tungsten trioxide (2D h-WO_3) is especially interesting because of its high sensitivity and selectivity to some gases. We firstly introduce the characteristics of 2D h-WO_3 gas sensing materials and discuss the effects of microstructure, oxygen vacancy, and doping modification on the gas sensing properties of 2D h-WO_3 mainly. Finally, we explore the application of 2D h-WO_3 gas sensing materials and propose some research directions.

Keywords: 2D, hexagonal WO_3, gas sensing, oxygen vacancy, metal oxide semiconductor

OPEN ACCESS

Edited by:
Zhaofu Zhang,
University of Cambridge,
United Kingdom

Reviewed by:
Nan Yang,
Xingtai University, China
Hao Luo,
Southwest University of Science and Technology, China
Xiaochuan Duan,
Taiyuan University of Technology, China
Qingkai Qian,
Chongqing University, China

****Correspondence:***
Shoubing Ding
shoubingding@cqnu.edu.cn
Zhimin Wu
zmwu@cqnu.edu.cn

Specialty section:
This article was submitted to Physical Chemistry and Chemical Physics, a section of the journal Frontiers in Chemistry

Received: *01 October 2021*
Accepted: *08 November 2021*
Published: *06 December 2021*

Citation:
Li Y, Zhou Q, Ding S and Wu Z (2021) Research Progress of Gas Sensing Performance of 2D Hexagonal WO_3. Front. Chem. 9:786607. doi: 10.3389/fchem.2021.786607

INTRODUCTION

As a critical component of the intelligent detection system, the gas sensor (Lee et al., 2018) has been widely used in environmental monitoring (Ji et al., 2019a), respiratory analysis, explosive gases, and automobile exhaust detection. Based on different working mechanisms, the developed gas sensors include semiconductor gas sensors (Morrison, 1987a; Zhang et al., 2021), polymer gas sensors (Zee and Judy, 2001), and electrochemical gas sensors (Tierney and Kim, 1993). Among them, the semiconductor gas sensors can also be divided into resistive and non-resistive types, while the resistive semiconductor gas sensors have advantages of high sensitivity and easy preparation (Seiyama et al., 1962). Meanwhile, compared with carbon and other organic gas sensing materials, the resistive metal oxide gas sensors (Nazemi et al., 2019) have become the research hotspot due to their high responsivity (Demarne and Grisel, 1988) and excellent selectivity (Morrison, 1987b). As a highly sensitive metal oxide gas sensing material, tungsten trioxide (WO_3) has attracted extensive attention because of its unique physical and chemical properties (Salje and Viswanathan, 1975), and its applications in photocatalysis (Dong et al., 2017) and electrochromic (Adhikari and Sarkar, 2014).

WO_3 is a typical metal oxide semiconductor with various phase transition structures, while different phases can induce different gas sensitivity. The stable structures at room temperature are m-WO_3 and h-WO_3. In recent years, as the most stable structure, m-WO_3 has attracted much attention (Hübner et al., 2010; Oison et al., 2011), but bulk m-WO_3 gas sensors are not sensitive to some gases at 25°C–500°C, such as CO (Ahsan et al., 2012) and H_2S (Szilágyi et al., 2010). Therefore, it is urgent to improve the gas sensitivity of WO_3 at room temperature effectively. Xu et al. (2008) found that the sensitivity of h-WO_3 almost linearly increases with CO concentration at room temperature. Szilágyi et al. (2010) found that h-WO_3 becomes more sensitive than m-WO_3 compared to m-WO_3 when the concentration of H_2S is 10 ppm. Meanwhile, the large hexagonal and trigonal tunnel structures of h-WO_3 result in it having a high specific surface area (as shown in **Figure 1**) (Balaji et al., 2009), indicating that h-WO_3 is an excellent candidate material for gas sensors.

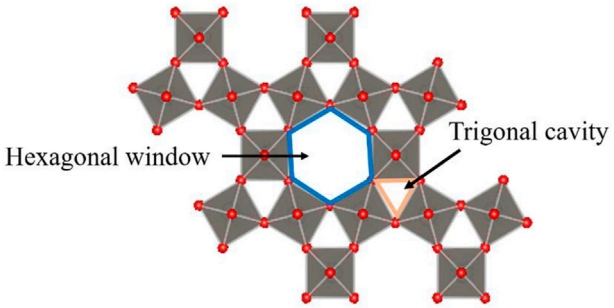

FIGURE 1 | The hexagonal window and trigonal cavity of the hexagonal WO_3(001) surface (Balaji et al., 2009).

To effectively improve the gas sensitivity of the material, various preparation methods have been used to prepare WO_3 nanomaterials on various dimensions (0D, 1D, 2D, and 3D) (Qin et al., 2010; Zhang et al., 2010; D'Arienzo et al., 2014). Among them, 2D nanomaterials are widely used because of their high specific surface area and abundant oxygen vacancies (Yang et al., 2016; Liu et al., 2017; Yang et al., 2017). The unique characteristics of 2D WO_3 nanostructure compared with the bulk material include (1) higher specific surface area, which will provide more interaction area between tested gases and gas sensor surface molecules; (2) quantum confinement effects, due to the inherently small size of nanostructure materials, that can significantly affect charge transport, electronic band structure, and optical properties (Zheng et al., 2011). Based on this, we mainly review the effects of microstructure, oxygen vacancy, and doping modification on the gas sensing performance of 2D h-WO_3 and explore the application prospect of the 2D h-WO_3 gas sensor.

CHARACTERISTICS OF 2D h-WO_3 GAS SENSING MATERIAL

As a kind of metal oxide semiconductor, 2D h-WO_3 gas sensing material has been an excellent candidate material for gas sensors due to its advantages of easy preparation, stable crystal structure, high specific surface area, and abundant oxygen vacancies.

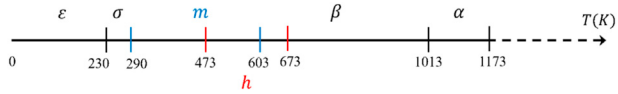

FIGURE 2 | Stability temperature domains of the different polymorphs of WO_3 (Gerand et al., 1979; Roussel et al., 2000).

Easy Preparation

Table 1 shows some typical preparation methods of 2D h-WO_3. Among them, the hydrothermal method is the most widely used. According to this method (Kitagawa et al., 2009; Szilágyi et al., 2010; Ji et al., 2019b), $(NH_4)_{10}W_{12}O_{41}{\cdot}5H_2O$ is firstly put into a high-pressure cauldron as the raw material. Then, under high temperature and high pressure, $(NH_4)_{10}W_{12}O_{41}{\cdot}5H_2O$ recrystallizes to obtain precipitates (h-WO_3 crystals). Finally, the precipitates are removed and washed several times with deionized water to obtain the final product. Compared with vapor/liquid phase deposition methods, the hydrothermal method is simple and economical, and can prepare nanomaterials with high purity, good chemical uniformity and high dispersion. 2D h-WO_3 is classified as the surface-controlled gas sensor by a gas sensing mechanism.

Stable Crystal Structure

The phases of WO_3 can transform when it is annealed under different conditions. However, it does not simply form new nanostructures, but the original WO_6 octahedron distorts and twists to a certain extent and thus can form different crystal phases. The phase transition with temperature of WO_3 is shown in **Figure 2** (Salje et al., 1997; Vogt et al., 1999; Roussel et al., 2000), which is monoclinic II (ε-WO_3 < −43°C) → triclinic (−43°C < σ-WO_3 < 17°C) → monoclinic I (17°C < m-WO_3 < 330°C) → orthorhombic (330°C < β-O_3 < 740°C) → tetragonal (740°C < α-WO_3). Meanwhile, Gerand et al. (1979) found that stable hexagonal WO_3 (h-WO_3) can be prepared by dehydration method at 200°C–400°C.

Tian et al. (2020) has calculated the gas (O_2) sensing on hexagonal WO_3 (001) surface by using the pseudopotentials method based on the density functional theory (DFT). The formation energy (E_{form}) of the h-WO_3 (001) monolayer is

TABLE 1 | The preparation methods and types of 2D h-WO_3.

Structure	Materials	Method	Gas	Type
2D h-WO_3	Nanosheet	Hydrothermal method	NH_3[a]	Surface-controlled gas sensor
	Nanosheet	Hydrothermal method	H_2S[b]	
	Film	Hydrothermal method	NO_2[c]	
	Film	Sol-gel polymerization	H_2[d]	
	Film	Acidic precipitation	NH_3[e]	

[a]*Ji et al.(2019b).*
[b]*Szilágyi et al.(201).*
[c]*Kitagawa et al.(2009).*
[d]*Zhang et al.(2019).*
[e]*Balázsi et al.(2008).*

TABLE 2 | The carrier mobility μ at T = 300 K.

Material	μ (10^3 cm^2 V^{-1} s^{-1})
h-WO_3 monolayer[a]	0.886
Graphene[b]	15.000
InP_3[c]	1.919
SnP_3[d]	7.150
GeP_3[e]	0.360
MoS_2[f]	0.201
2D MoS_2 flake[g]	0.600
SnO_2 bulk[h]	0.160
WO_3 bulk[h]	0.010

[a]*Sone et al.(2018).*
[b]*Novoselov et al.(2004).*
[c]*Miao et al.(2017).*
[d]*Ghosh et al.(2018).*
[e]*Gerand et al.(1979).*
[f]*Cai et al.(2014).*
[g]*Alsaif et al.(2016).*
[h]*Yamazoe et al.(2003).*

−5.87 eV, indicating that the h-WO_3 (001) monolayer is stable. The carrier mobility μ calculated from the energy band is 886 $cm^2V^{-1}s^{-1}$ (as shown in **Table 2**) at T = 300 K. The value is higher than that of 2D GeP_3 (Gerand et al., 1979) and MoS_2 (Cai et al., 2014) and is about 88 times higher than that of bulk WO_3 (Yamazoe et al., 2003), which implies that 2D h-WO_3 may have excellent gas sensing performance.

High Specific Surface Area

Sun et al. (2015) investigated the high surface area tunnels in 3D h-WO_3 by low-pressure CO_2 adsorption isotherms with nonlocal density functional theory fitting (NLDET), transmission electron microscopy (TEM), and thermal gravimetric analysis. They found that h-WO_3 has a large hexagonal tunnel structure (the diameter is 3.67 Å) and high specific surface area (45.585 m^2/g). Meanwhile, the large lateral size and ultrathin thickness of 2D materials provide it with ultrahigh specific surface areas and high ratios of exposed surface atoms (Zhang, 2015), significantly improving the gas sensing performance of 2D h-WO_3.

Abundant Oxygen Vacancies

The conduction band of 2D WO_3 mainly consists of W-5d electrons, and the valence band mainly consists of O-2p electrons (Niklasson et al., 2004). Chatten et al. (2005) found that abundant oxygen vacancies are related to the energy gap between O-2p and W-5d orbitals in non-stoichiometric tungsten oxide. Makarov and Trontelj (1996) pointed out that the oxygen vacancies in 2D WO_3 can affect the conductivity and carrier concentration, and further affect the gas sensing performance of WO_3. For example, Tian et al. (2020) found that oxygen vacancies provide electrons to O_2 gas molecules on the WO-terminated h-WO_3 (001) surface, thus effectively improving the gas sensing performance of h-WO_3 (001) surface to O_2.

INFLUENCING FACTORS OF 2D h-WO_3 ON GAS SENSING PERFORMANCE

When the gas sensors are exposed to the air, O_2 molecules are physically or chemically adsorbed on the surface of 2D h-WO_3. The oxygen will be dissociated and capture the electrons from the conduction bands of 2D h-WO_3, generating ionized oxygen species (mainly O^-). This leads to a decrease in the number of electrons on the surface and forming an electron depletion region (EDR), which causes the first change in resistance. When the sensors are exposed to the target gas, the gas molecules are adsorbed on the surface of 2D h-WO_3. Then, the gas molecules react with pre-absorbed oxygen and change the number of the electrons of ionized oxygen species, increasing the density of carriers in the 2D h-WO_3. It results in the second change in resistance (Deng et al., 2015; Li et al., 2015; Liu et al., 2016).

Effect of Microstructure on Gas Sensing Performance of 2D h-WO_3

Figure 3 shows different microstructures of h-WO_3. It can be seen that h-WO_3 nanosheets and films can provide more gas molecular absorption sites because of their obvious orientation, small particle size, large specific surface area, and no agglomeration. However, h-WO_3 nanoparticles, nanowires, and nanospheres have a negative effect on gas transportation and reaction due to serious agglomeration or large particle size. Moreover, we also find from **Table 3** that h-WO_3 nanosheets and films have the highest responsiveness (R) and wider detection scope (S) to H_2, NH_3, H_2S, and NO_2, compared with nanowires, nanorods, nanospheres, and nanoparticles. Different h-WO_3 nanomaterials have exhibited different gas sensing performance due to their different microstructures. Among them, 2D h-WO_3 nanomaterials show important application prospects in the gas sensing field due to their excellent gas sensing performance.

Effect of Oxygen Vacancy on Gas Sensing Performance of 2D h-WO_3

In 1964, Kevane (1964) found that oxygen vacancies are easy to form in the preparation of metal oxide semiconductors. Makarov and Trontelj (1996) found that the oxygen vacancies would affect the conductivity, thus further affecting the gas sensing performance of WO_3. However, the expression of oxygen vacancy on metal oxide semiconductor surfaces is not in agreement (Gillet et al., 2003). Until 2018, Tian et al. (2018) established a theory based on surface oxygen density (do) and unitedly expressed the oxygen vacancies on the WO_3 surface (**Table 4**). The O-terminated and WO-terminated h-WO_3 (001) surfaces with and without oxygen vacancy are denoted as O- for O-terminated, Vac O- for defective O-terminated, WO- for WO-terminated, and Vac WO- for defective WO-terminated, respectively. The surface oxygen densities are defined as d_o = 1, 1 > d_o > 0, d_o = 0, 0 > d_o > −1. Based on this, oxygen vacancies of the 2D h-WO_3 surface can be expressed by surface oxygen density.

Recently, Tian et al. (2014) investigated the effect of oxygen vacancy on the gas sensing performance of CO on 2D h-WO_3 (001) surface by using the first-principles calculations (**Table 5**). They found that the adsorption energy and charge transfer of CO of the defective O-terminated h-WO_3 (001) surface decrease by

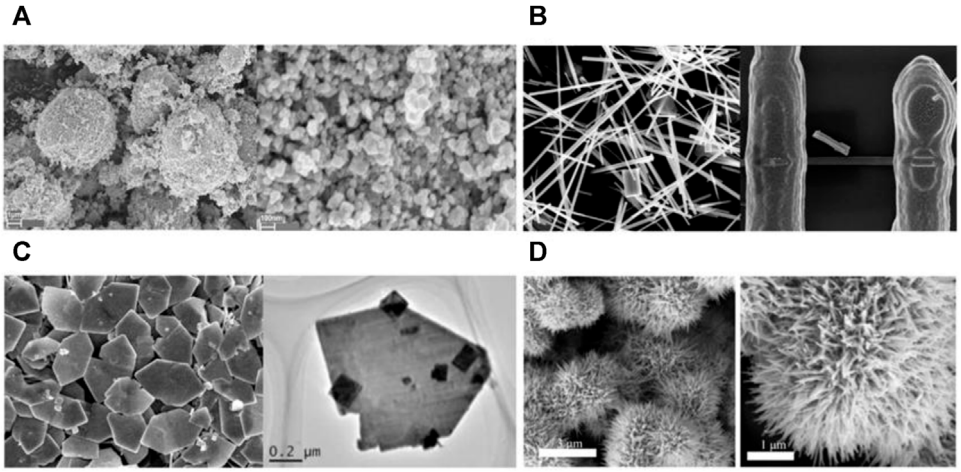

FIGURE 3 | The microstructure of h-WO_3 nanoparticle, nanowire, film, and nanosphere **(A)** 0D h-WO_3 nanoparticle (Szilágyi et al., 2010). **(B)** 1D h-WO_3 nanowire (Liu et al., 2014). **(C)** 2D h-WO_3 film (Meng et al., 2015). **(D)** 3D h-WO_3 nanosphere (Zhang et al., 2019).

TABLE 3 | Relationship between microstructure, particle size, and gas sensitivity of H_2, NH_3, H_2S, and NO_2 in h-WO_3 (*S* is the detection scope, *R* is the responsiveness, and *C* is concentration).

Gas	Material	Size/nm	T/°C	S/ppm	R	
					$R = R_a/R_g$	C/ppm
	Film[a]	110–320	450	200	151.9	200
H_2	Nanoflower[b]	450–600	270	100	2.5–5	100
	Nanosphere[c]	500–2000	250	10–80	0–5	80
	Nanoparticle[d]	50–100	300	10–50	5–5.5	50
NH_3	Nanorod[e]	30–100	400	50–200	22.5	200
	Nanosheet[f]	50–350	350	50–250	36.3	100
	Nanoparticle[g]	50–100	200	—	—	200
H_2S	Nanowire[h]	50–500	20	—	—	—
	Nanosheet[i]	—	330	0–40	45.86	40
	Nanoparticle[j]	700–1,000	75	1–10	5.8	10
NO_2	Film[k]	1,000–2000	200	0.01–0.5	10^4	0–0.1
	Nanosphere[l]	500–2000	250	10–80	60–65	80

[a]*Sone et al.(2018).*
[b]*Zhang et al.(2019).*
[c]*Wei et al.(2017).*
[d]*Wang et al.(2007).*
[e]*Szilágyi et al.(2009).*
[f]*Ji et al.(2019b).*
[g]*Liu et al.(2014).*
[h]*Shi et al.(2016).*
[i]*Szilágyi et al.(2010).*
[j]*Meng et al.(2015).*
[k]*Kitagawa et al.(2009).*
[l]*Zhang et al.(2019).*

0.68 eV and 0.002e, respectively, compared with the O-terminated h-WO_3 (001) surface. For defective WO-terminated, the values of decrease are 0.4 eV and 0.011e, respectively. The result shows that the adsorption and sensing ability of CO on the defective O- and WO-terminated h-WO_3 (001) surface decreases. The oxygen vacancy inhibits the oxidation reaction of reducing gas CO on the 2D h-WO_3 (001) surface, which reduces the gas sensing performance of the 2D h-WO_3.

TABLE 4 | The relationship between surface oxygen vacancy and oxygen density of 2D h-WO_3 (Tian et al., 2018).

2D h-WO_3(001)	Surface oxygen density d_o
O-	1
Vac O-	$1 > d_o > 0$
WO-	0
Vac WO-	$0 > d_o > -1$

Oxygen vacancy also inhibits the gas sensing performance of other reducing gases (H_2S, CH_4, H_2) on the 2D h-WO_3 (001) surface (Szilágyi et al., 2010; Tian et al., 2017; Wu et al., 2019) (**Table 5**). However, the inhibitory effect of oxygen vacancy on H_2S and CH_4 is unapparent. Although the gas sensing performance of H_2S is inhibited by oxygen vacancy, the value (1.85 eV) is still large enough for effective adsorption of H_2S on the surface. The adsorption sensing ability of CH_4 on the 2D h-WO_3 (001) surface is weak and the inhibition of oxygen vacancy makes it difficult to spontaneously adsorb on defective WO-terminated h-WO_3 (001) surface. Moreover, oxygen vacancy has the strongest inhibitory effect on the gas sensing performance of H_2 on the 2D h-WO_3 (001) surface. The adsorption energy decreases from 2.62 to 0.16 eV and the charge transfer decreases from 0.635e to 0.065e. The gas adsorption ability of H_2 on the 2D h-WO_3 (001) surface greatly reduces with the decrease of surface oxygen density.

More recently, Tian et al. (2020) investigated the effect of oxygen vacancy on the gas sensing performance of O_2 on the 2D h-WO_3 (001) surface (**Table 5**) by the first principles with pseudopotentials method based on the DFT. They found that the adsorption energy of O_2 of the defective O-terminated h-WO_3 (001) surface increases by 0.05 eV and the charge transfer decreases by 0.104e compared with the O-terminated h-WO_3 (001) surface. For the defective WO-terminated surface, the values of increase are 5.65 eV and 0.077e, relatively. The result

TABLE 5 | The adsorption energy and charge transfer of O_2, CO, H_2, H_2S, and CH_4 on 2D h-WO_3 (001) surface with oxygen vacancy (d_o is surface oxygen density, C is charge transfer, ΔC is the variation of charge transfer, ↑ is promotion, ↓ is reduction).

Gas	d_o	Configurations	E_{ads}/eV	ΔE_{ads}/eV	C/e	ΔC/e	Effect
CO[a]	1	OC-O_{1c}	2.64	0	0.5	0	—
	$1 > d_o > 0$	OC-O_{1c}	1.96	−0.68	0.498	−0.002	↓
	0	OC-W_{5c}	0.97	0	0.14	0	—
	$0 > d_o > -1$	OC-W_{5c}	0.57	−0.4	-0.129	−0.011	↓
H_2S[b]	1	H_2S/Pt_4	2.78	0	0.483	0	—
	$1 > d_o > 0$	H_2S/Pt_2	1.85	−0.93	0.474	−0.009	↓
H_2[c]	1	H_2-O_{1c}-P	2.62	0	0.635	0	—
	$1 > d_o > 0$	H_2-Pre-O_{1c}	0.60	−2.02	0.621	−0.014	↓
	0	H_2-O_{2c}-P_1	0.19	0	0.09	0	—
	$0 > d_o > -1$	H_2-W_{4c}-P	0.16	−0.03	0.065	−0.025	↓
CH_4[d]	1	H_2CH_2-O_{1c}	0.12	0	0.012	0	—
	$1 > d_o > 0$	HCH_3-W_{5c}	0.18	−0.06	0.049	+0.037	↓
	0	H_2CH_2-W_{5c}	0.11	0	0.01	0	—
	$0 > d_o > -1$	—	−6.15	—	—	—	↓
O_2[e]	1	O_2-O_{1c}-P	0.19	0	0.198	0	—
	$1 > d_o > 0$	O_2-W_{5c}-P	0.24	+0.05	−0.094	−0.104	↑
	0	O_2-O_{1c}-V	1.65	0	−0.389	0	—
	$0 > d_o > -1$	O_2-Vac-V	7.30	+5.65	−0.466	+0.077	↑

[a]*Tian et al. (2014).*
[b]*Szilágyi et al.(2010).*
[c]*Tian et al.(2017).*
[d]*Wu et al.(2019).*
[e]*Tian et al.(2020).*

shows that the adsorption and sensing ability of O_2 are improved on the defective O- and WO-terminated h-WO_3 (001) surface. The oxygen vacancy activates the O-O bond of O_2 and promotes the reduction reaction of oxidizing gas O_2 on the 2D h-WO_3 (001) surface, which improves the gas sensing performance of the 2D h-WO_3.

These results indicate that the effect of oxygen vacancy on gases with different redox properties is different. For reducing gases, the oxygen vacancy inhibits their oxidation reactions on the 2D h-WO_3 (001) surface and then reduces the gas sensing performance of the reducing gases. On the contrary, for oxidizing gases, the oxygen vacancy promotes the reduction reaction and then improves the gas sensing performance.

Effect of Doping Modification on Gas Sensing Performance of 2D h-WO_3

Various methods have been performed to improve the gas sensing performance, to overcome the defects of pure metal oxides such as low sensitivity, low selectivity, and long response time for some gases (Liu et al., 2019). Among them, noble metal doping is one of the most common and effective methods. Due to the high electronic activity of noble metal elements, the activation energy of the reaction can be reduced during the contact reaction between the gas sensing material and the target gas, thus improving the gas sensing performance of the materials (Xu et al., 1990) when they react with target gases. Based on this, noble metals such as Au, Ag, Pd, and Pt are usually doped on WO_3 films to improve their sensitivity and selectivity to NO_x (Penza et al., 1998; Chen and Tsang, 2003), H_2S (Stankova et al., 2004; Hurtado-Aular et al., 2021), CH_3COCH_3 (Feng et al., 2021), etc.

TABLE 6 | Adsorption energy and charge transfer of CO and H_2S on noble metal doped 2D h-WO_3 (001) surface.

Gas	Surface	E_{ads}/eV	Charge transfer/e
CO[a]	Clean	−0.69	+0.08
	Cu	−1.79	+0.02
	Ag	−0.97	+0.04
	Au	−2.06	+0.07

[a]*Hurtado-Aular et al.(2021).*

Recently, the gas sensing performance of CO adsorption on the 2D h-WO_3 (001) surface doped with noble metals Cu, Ag, and Au were investigated by using DFT (as shown in **Table 6**) (Hurtado-Aular et al., 2021). They found that the incorporation of Au and Cu atoms improves the surface activity of the material and the absorptivity of CO on the 2D h-WO_3 (001) surface. Meanwhile, the doped Au and Cu atoms provide a large number of electrons. The charge transfer increases, which effectively improves the sensing performance of CO on the 2D h-WO_3 (001) surface.

Theoretically, noble metal doping promotes the adsorption and sensing ability of the target gas on 2D h-WO_3 surface, and then improves the gas sensing performance of 2D h-WO_3. However, the experimental study on the mechanism of improving the gas sensing performance of noble metal doped h-WO_3 films is still insufficient.

SUMMARY AND PROSPECT

The research progress of the gas sensing performance of 2D h-WO_3 has been reviewed. Firstly, we briefly summarize the

characteristics of 2D h-WO_3 gas sensing materials. Then, the effects of microstructure, oxygen vacancy, and doped metal on the performance of 2D h-WO_3 gas sensors are mainly discussed. We find that the 2D h-WO_3 gas sensor has better gas sensing performance than other WO_3 nanomaterials due to their small particle size and large specific surface area. Moreover, the effect of oxygen vacancy on the gas sensitivity of different oxidation-reducing gases on 2D h-WO_3 is different. Besides, we also note that noble metal doping can improve the gas sensing performance of 2D h-WO_3 due to the high electronic activity of noble metals and the reduction of reaction activation energy.

As we all know, 2D h-WO_3 is an excellent candidate material for metal oxide semiconductor gas sensors, which has vital research significance and wide application prospects in gas sensors. However, there are still some unsolved problems in 2D h-WO_3 that need to be completely solved, such as the low sensitivity and low selectivity to some gases. To solve the above problems, the possible solutions include the following: (1) Photoactivation method (i.e., activation of reactants by light), which can improve the sensitivity and selectivity effectively. Deng et al. (2012) activated mesoporous WO_3 sensing material and improved the sensitivity of WO_3 to HCHO by using visible light irradiation at room temperature. Moreover, Trawka et al. (2016) enhanced the sensitivity and selectivity of WO_3-based gas sensors greatly by ultraviolet irradiation. (2) Noble metal doping method improves sensitivity and selectivity. Adding precious metal catalysts has become an important method to improve the gas sensing performance of metal oxide semiconductors, because the catalyst has a great influence on the resistance and sensitivity of semiconductor gas sensing materials (Krebs and Grisel, 1993).

AUTHOR CONTRIBUTIONS

All authors listed have made a substantial, direct, and intellectual contribution to the work, and approved it for publication.

FUNDING

The work described in this paper is supported by Chongqing Natural Science Foundation of China (Grant No. cstc2019jcyj-msxmX0251), the Science and Technology Research Program of Chongqing Education Commission of China (Grant No. KJQN202000505), the Doctoral Fund Project of Chongqing Normal University (Grant No. 20XLB001), and the undergraduate innovation and entrepreneurship training program of Chongqing (Grant No. S202110637121).

REFERENCES

Adhikari, S., and Sarkar, D. (2014). High Efficient Electrochromic WO_3 Nanofibers. *Electrochimica Acta* 138, 115–123. doi:10.1016/j.electacta.2014.06.062

Ahsan, M., Tesfamichael, T., Ionescu, M., Bell, J., and Motta, N. (2012). Low Temperature CO Sensitive Nanostructured WO_3 Thin Films Doped with Fe. *Sensors Actuators B: Chem.* 162 (1), 14–21. doi:10.1016/j.snb.2011.11.038

Alsaif, M. M. Y. A., Chrimes, A. F., Daeneke, T., Balendhran, S., Bellisario, D. O., Son, Y., et al. (2016). High-Performance Field Effect Transistors Using Electronic Inks of 2D Molybdenum Oxide Nanoflakes. *Adv. Funct. Mater.* 26 (1), 91–100. doi:10.1002/adfm.201503698

Balaji, S., Djaoued, Y., Albert, A.-S., Ferguson, R. Z., and Brüning, R. (2009). Hexagonal Tungsten Oxide Based Electrochromic Devices: Spectroscopic Evidence for the Li Ion Occupancy of Four-Coordinated Square Windows. *Chem. Mater.* 21 (7), 1381–1389. doi:10.1021/cm8034455

Balázsi, C., Wang, L., Zayim, E. O., Szilágyi, I. M., Sedlacková, K., Pfeifer, J., et al. (2008). Nanosize Hexagonal Tungsten Oxide for Gas Sensing Applications. *J. Eur. Ceram. Soc.* 28 (5), 913–917. doi:10.1016/j.jeurceramsoc.2007.09.001

Cai, Y., Zhang, G., and Zhang, Y.-W. (2014). Polarity-Reversed Robust Carrier Mobility in Monolayer MoS_2 Nanoribbons. *J. Am. Chem. Soc.* 136 (17), 6269–6275. doi:10.1021/ja4109787

Chatten, R., Chadwick, A. V., Rougier, A., and Lindan, P. J. D. (2005). The Oxygen Vacancy in Crystal Phases of WO_3. *J. Phys. Chem. B* 109 (8), 3146–3156. doi:10.1021/jp045655r

Chen, L., and Tsang, S. C. (2003). Ag Doped WO_3-Based Powder Sensor for the Detection of NO Gas in Air. *Sensors Actuators B: Chem.* 89 (1), 68–75. doi:10.1016/S0925-4005(02)00430-6

D'Arienzo, M., Armelao, L., Mari, C. M., Polizzi, S., Ruffo, R., Scotti, R., et al. (2014). Surface Interaction of WO_3 Nanocrystals with NH_3. Role of the Exposed crystal Surfaces and Porous Structure in Enhancing the Electrical Response. *RSC Adv.* 4 (22), 11012–11022. doi:10.1039/C3RA46726K

Demarne, V., and Grisel, A. (1988). An Integrated Low-Power Thin-Film CO Gas Sensor on Silicon. *Sensors and Actuators* 13 (4), 301–313. doi:10.1016/0250-6874(88)80043-X

Deng, J., Zhang, R., Wang, L., Lou, Z., and Zhang, T. (2015). Enhanced Sensing Performance of the Co_3O_4 Hierarchical Nanorods to NH_3 Gas. *Sensors Actuators B: Chem.* 209, 449–455. doi:10.1016/j.snb.2014.11.141

Deng, L., Ding, X., Zeng, D., Tian, S., Li, H., and Xie, C. (2012). Visible-light Activate Mesoporous WO_3 Sensors with Enhanced Formaldehyde-Sensing Property at Room Temperature. *Sensors Actuators B: Chem.* 163 (1), 260–266. doi:10.1016/j.snb.2012.01.049

Dong, P., Hou, G., Xi, X., Shao, R., and Dong, F. (2017). WO_3-based Photocatalysts: Morphology Control, Activity Enhancement and Multifunctional Applications. *Environ. Sci. Nano* 4 (3), 539–557. doi:10.1039/C6EN00478D

Feng, D.-L., Zhu, Z.-Y., Du, L.-L., Xing, X.-X., Wang, C., Chen, J., et al. (2021). Improved Sensing Performance of WO_3 Nanoparticles Decorated with Ag and Pt Nanoparticles. *Rare Met.* 40 (6), 1642–1650. doi:10.1007/s12598-020-01666-0

Gerand, B., Nowogrocki, G., Guenot, J., and Figlarz, M. (1979). Structural Study of a New Hexagonal Form of Tungsten Trioxide. *J. Solid State. Chem.* 29 (3), 429–434. doi:10.1016/0022-4596(79)90199-3

Ghosh, B., Puri, S., Agarwal, A., and Bhowmick, S. (2018). SnP_3: A Previously Unexplored Two-Dimensional Material. *J. Phys. Chem. C* 122 (31), 18185–18191. doi:10.1021/acs.jpcc.8b06668

Gillet, M., Lemire, C., Gillet, E., and Aguir, K. (2003). The Role of Surface Oxygen Vacancies upon WO_3 Conductivity. *Surf. Sci.* 532-535, 519–525. doi:10.1016/S0039-6028(03)00477-1

Hübner, M., Simion, C. E., Haensch, A., Barsan, N., and Weimar, U. (2010). CO Sensing Mechanism with WO_3 Based Gas Sensors. *Sensors Actuators B: Chem.* 151 (1), 103–106. doi:10.1016/j.snb.2010.09.040

Hurtado-Aular, O., Añez, R., and Sierraalta, A. (2021). DFT+U Study of the Electronic Structure Changes of WO_3 Monoclinic and Hexagonal Surfaces upon Cu, Ag, and Au Adsorption. Applications for CO Adsorption. *Surf. Sci.* 714, 121907. doi:10.1016/j.susc.2021.121907

Ji, H., Zeng, W., and Li, Y. (2019a). Gas Sensing Mechanisms of Metal Oxide Semiconductors: a Focus Review. *Nanoscale* 11 (47), 22664–22684. doi:10.1039/C9NR07699A

Ji, H., Zeng, W., Xu, Y., and Li, Y. (2019b). Nanosheet-assembled Hierarchical WO_3 Flower-like Nanostructures: Hydrothermal Synthesis and NH_3-sensing Properties. *Mater. Lett.* 250, 155–158. doi:10.1016/j.matlet.2019.05.023

Kevane, C. J. (1964). Oxygen Vacancies and Electrical Conduction in Metal Oxides. *Phys. Rev.* 133 (5A), A1431–A1436. doi:10.1103/PhysRev.133.A1431

Kitagawa, C., Takahashi, A., Okochi, Y., and Tamaki, J. J. S. (2009). WO_3 Crystals and Their NO_2-Sensing Properties. *Sensors Mater.* 21 (5), 259–264. doi:10.18494/SAM.2009.611

Krebs, P., and Grisel, A. (1993). A Low Power Integrated Catalytic Gas Sensor. *Sensors Actuators B: Chem.* 13 (1), 155–158. doi:10.1016/0925-4005(93)85349-F

Lee, E., Yoon, Y. S., and Kim, D.-J. (2018). Two-Dimensional Transition Metal Dichalcogenides and Metal Oxide Hybrids for Gas Sensing. *ACS Sens.* 3 (10), 2045–2060. doi:10.1021/acssensors.8b01077

Li, L., Zhang, C., and Chen, W. (2015). Fabrication of SnO_2-SnO Nanocomposites with P-N Heterojunctions for the Low-Temperature Sensing of NO_2 Gas. *Nanoscale* 7 (28), 12133–12142. doi:10.1039/C5NR02334C

Liu, B., Tang, D., Zhou, Y., Yin, Y., Peng, Y., Zhou, W., et al. (2014). Electrical Characterization of H_2S Adsorption on Hexagonal WO_3 Nanowire at Room Temperature. *J. Appl. Phys.* 116 (16), 164310. doi:10.1063/1.4898127

Liu, T., Liu, J., Hao, Q., Liu, Q., Jing, X., Zhang, H., et al. (2016). Porous Tungsten Trioxide Nanolamellae with Uniform Structures for High-Performance Ethanol Sensing. *CrystEngComm* 18 (43), 8411–8418. doi:10.1039/C6CE01587E

Liu, W., Qu, Y., Li, H., Ji, F., Dong, H., Wu, M., et al. (2019). Nanostructure Bi_2WO_6: Surfactant-Assisted Hydrothermal Synthesis for High Sensitive and Selective Sensing of H_2S. *Sensors Actuators B: Chem.* 294, 224–230. doi:10.1016/j.snb.2019.05.042

Liu, X., Ma, T., Pinna, N., and Zhang, J. (2017). Two-Dimensional Nanostructured Materials for Gas Sensing. *Adv. Funct. Mater.* 27 (37), 1702168. doi:10.1002/adfm.201702168

Makarov, V. O., and Trontelj, M. (1996). Sintering and Electrical Conductivity of Doped WO_3. *J. Eur. Ceram. Soc.* 16 (7), 791–794. doi:10.1016/0955-2219(95)00204-9

Meng, Z., Fujii, A., Hashishin, T., Wada, N., Sanada, T., Tamaki, J., et al. (2015). Morphological and crystal Structural Control of Tungsten Trioxide for Highly Sensitive NO_2 Gas Sensors. *J. Mater. Chem. C* 3 (5), 1134–1141. doi:10.1039/C4TC02762K

Miao, N., Xu, B., Bristowe, N. C., Zhou, J., and Sun, Z. (2017). Tunable Magnetism and Extraordinary Sunlight Absorbance in Indium Triphosphide Monolayer. *J. Am. Chem. Soc.* 139 (32), 11125–11131. doi:10.1021/jacs.7b05133

Morrison, S. R. (1987a). Mechanism of Semiconductor Gas Sensor Operation. *Sensors and Actuators* 11 (3), 283–287. doi:10.1016/0250-6874(87)80007-0

Morrison, S. R. (1987b). Selectivity in Semiconductor Gas Sensors. *Sensors and Actuators* 12 (4), 425–440. doi:10.1016/0250-6874(87)80061-6

Nazemi, H., Joseph, A., Park, J., and Emadi, A. (2019). Advanced Micro- and Nano-Gas Sensor Technology: A Review. *Sensors* 19 (6), 1285. doi:10.3390/s19061285

Niklasson, G. A., Berggren, L., and Larsson, A.-L. (2004). Electrochromic Tungsten Oxide: the Role of Defects. *Solar Energ. Mater. Solar Cell* 84 (1), 315–328. doi:10.1016/j.solmat.2004.01.045

Novoselov, K. S., Geim, A. K., Morozov, S. V., Jiang, D., Zhang, Y., Dubonos, S. V., et al. (2004). Electric Field Effect in Atomically Thin Carbon Films. *Science* 306 (5696), 666–669. doi:10.1126/science.1102896

Oison, V., Saadi, L., Lambert-Mauriat, C., and Hayn, R. (2011). Mechanism of CO and O_3 Sensing on WO_3 Surfaces: First Principle Study. *Sensors Actuators B: Chem.* 160 (1), 505–510. doi:10.1016/j.snb.2011.08.018

Penza, M., Martucci, C., and Cassano, G. (1998). NO_x Gas Sensing Characteristics of WO_3 Thin Films Activated by noble Metals (Pd, Pt, Au) Layers. *Sensors Actuators B: Chem.* 50 (1), 52–59. doi:10.1016/S0925-4005(98)00156-7

Qin, Y., Hu, M., and Zhang, J. (2010). Microstructure Characterization and NO_2-Sensing Properties of Tungsten Oxide Nanostructures. *Sensors Actuators B: Chem.* 150 (1), 339–345. doi:10.1016/j.snb.2010.06.063

Roussel, P., Labbé, P., and Groult, D. (2000). Symmetry and Twins in the Monophosphate Tungsten Bronze Series $(PO_2)_4(WO_3)_{2m}$ $(2 \leq M \leq 14)$. *Acta Crystallogr. Sect B* 56 (3), 377–391. doi:10.1107/S0108768199016195

Salje, E. K. H., Rehmann, S., Pobell, F., Morris, D., Knight, K. S., Herrmannsdörfer, T., et al. (1997). Crystal Structure and Paramagnetic Behaviour of. *J. Phys. Condens. Matter* 9 (31), 6563–6577. doi:10.1088/0953-8984/9/31/010

Salje, E., and Viswanathan, K. (1975). Physical Properties and Phase Transitions in WO_3. *Acta Cryst. Sect A.* 31 (3), 356–359. doi:10.1107/S0567739475000745

Seiyama, T., Kato, A., Fujiishi, K., and Nagatani, M. (1962). A New Detector for Gaseous Components Using Semiconductive Thin Films. *Anal. Chem.* 34 (11), 1502–1503. doi:10.1021/ac60191a001

Shi, J., Cheng, Z., Gao, L., Zhang, Y., Xu, J., and Zhao, H. (2016). Facile Synthesis of Reduced Graphene Oxide/hexagonal WO_3 Nanosheets Composites with Enhanced H2S Sensing Properties. *Sensors Actuators B: Chem.* 230, 736–745. doi:10.1016/j.snb.2016.02.134

Sone, B. T., Nkosi, S. S., Nkosi, M. M., Coetsee-Hugo, E., Swart, H. C., and Maaza, M. (2018). Self-assembled Micro-/nanostructured WO_3 Thin Films by Aqueous Chemical Growth and Their Applications in H_2 and CO_2 Sensing. *AIP Conf. Proc.* 1962 (1), 040003. doi:10.1063/1.5035541

Stankova, M., Vilanova, X., Calderer, J., Llobet, E., Ivanov, P., Gràcia, I., et al. (2004). Detection of SO_2 and H_2S in CO_2 Stream by Means of WO_3-Based Micro-hotplate Sensors. *Sensors Actuators B: Chem.* 102 (2), 219–225. doi:10.1016/j.snb.2004.04.030

Sun, W., Yeung, M. T., Lech, A. T., Lin, C.-W., Lee, C., Li, T., et al. (2015). High Surface Area Tunnels in Hexagonal WO_3. *Nano Lett.* 15 (7), 4834–4838. doi:10.1021/acs.nanolett.5b02013

Szilágyi, I. M., Saukko, S., Mizsei, J., Tóth, A. L., Madarász, J., and Pokol, G. (2010). Gas Sensing Selectivity of Hexagonal and Monoclinic WO_3 to H_2S. *Solid State. Sci.* 12 (11), 1857–1860. doi:10.1016/j.solidstatesciences.2010.01.019

Szilágyi, I. M., Wang, L., Gouma, P.-I., Balázsi, C., Madarász, J., and Pokol, G. (2009). Preparation of Hexagonal WO_3 from Hexagonal Ammonium Tungsten Bronze for Sensing NH_3. *Mater. Res. Bull.* 44 (3), 505–508. doi:10.1016/j.materresbull.2008.08.003

Tian, F. H., Gong, C., Peng, Y., and Xue, X. (2017). H_2 Sensing Mechanism under Different Oxygen Concentration on the Hexagonal WO_3 (001) Surface: A Density Functional Theory Study. *Sensors Actuators B: Chem.* 244, 655–663. doi:10.1016/j.snb.2016.12.035

Tian, F. H., Gong, C., Wu, R., and Liu, Z. (2018). Oxygen Density Dominated Gas Sensing Mechanism Originated from CO Adsorption on the Hexagonal WO_3 (001) Surface. *Mater. Today Chem.* 9, 28–33. doi:10.1016/j.mtchem.2018.04.004

Tian, F. H., Liu, Z., Tian, J., and Zhang, Y. (2020). Oxygen Vacancy O-Terminated Surface: The Most Exposed Surface of Hexagonal WO_3 (001) Surface. *Chin. Chem. Lett.* 31 (8), 2095–2098. doi:10.1016/j.cclet.2020.01.015

Tian, F., Zhao, L., Xue, X.-Y., Shen, Y., Jia, X., Chen, S., et al. (2014). DFT Study of CO Sensing Mechanism on Hexagonal WO_3 (001) Surface: The Role of Oxygen Vacancy. *Appl. Surf. Sci.* 311, 362–368. doi:10.1016/j.apsusc.2014.05.069

Tierney, M. J., and Kim, H. O. L. (1993). Electrochemical Gas Sensor with Extremely Fast Response Times. *Anal. Chem.* 65 (23), 3435–3440. doi:10.1021/ac00071a017

Trawka, M., Smulko, J., Hasse, L., Granqvist, C.-G., Annanouch, F. E., and Ionescu, R. (2016). Fluctuation Enhanced Gas Sensing with WO_3-Based Nanoparticle Gas Sensors Modulated by UV Light at Selected Wavelengths. *Sensors Actuators B: Chem.* 234, 453–461. doi:10.1016/j.snb.2016.05.032

Vogt, T., Woodward, P. M., and Hunter, B. A. (1999). The High-Temperature Phases of WO_3. *J. Solid State. Chem.* 144 (1), 209–215. doi:10.1006/jssc.1999.8173

Wang, L., Pfeifer, J., Balázsi, C., and Gouma, P. I. (2007). Synthesis and Sensing Properties to NH3of Hexagonal WO_3 Metastable Nanopowders. *Mater. Manufacturing Process.* 22 (6), 773–776. doi:10.1080/10426910701385440

Wei, S., Zhao, J., Hu, B., Wu, K., Du, W., and Zhou, M. (2017). Hydrothermal Synthesis and Gas Sensing Properties of Hexagonal and Orthorhombic WO_3 Nanostructures. *Ceramics Int.* 43 (2), 2579–2585. doi:10.1016/j.ceramint.2016.11.064

Wu, R., Tian, F., Liu, Z., Xue, X., Zhang, J., and Zu, J. (2019). CH_4 Activation and Sensing on Hexagonal WO_3 (001) and (110) Surfaces. *Appl. Surf. Sci.* 481, 1154–1159. doi:10.1016/j.apsusc.2019.03.094

Xu, Y., Tang, Z., Zhang, Z., Ji, Y., and Zhou, Z. (2008). Large-Scale Hydrothermal Synthesis of Tungsten Trioxide Nanowires and Their Gas Sensing Properties. *Sen Lett.* 6 (6), 938–941. doi:10.1166/sl.2008.534

Xu, Z., Vetelino, J. F., Lec, R., and Parker, D. C. (1990). Electrical Properties of Tungsten Trioxide Films. *J. Vacuum Sci. Technol. A: Vacuum, Surf. Films* 8 (4), 3634–3638. doi:10.1116/1.576517

Yamazoe, N., Sakai, G., and Shimanoe, K. (2003). Oxide Semiconductor Gas Sensors. *Catal. Surv. Asia* 7 (1), 63–75. doi:10.1023/A:1023436725457

Yang, S., Jiang, C., and Wei, S.-h. (2017). Gas Sensing in 2D Materials. *Appl. Phys. Rev.* 4 (2), 021304. doi:10.1063/1.4983310

Yang, W., Gan, L., Li, H., and Zhai, T. (2016). Two-dimensional Layered Nanomaterials for Gas-Sensing Applications. *Inorg. Chem. Front.* 3 (4), 433–451. doi:10.1039/C5QI00251F

Zee, F., and Judy, J. W. (2001). Micromachined Polymer-Based Chemical Gas Sensor Array. *Sensors Actuators B: Chem.* 72 (2), 120–128. doi:10.1016/S0925-4005(00)00638-9

Zhang, C., Debliquy, M., Boudiba, A., Liao, H., and Coddet, C. (2010). Sensing Properties of Atmospheric Plasma-Sprayed WO_3 Coating for Sub-ppm NO_2 Detection. *Sensors Actuators B: Chem.* 144 (1), 280–288. doi:10.1016/j.snb.2009.11.006

Zhang, H. (2015). Ultrathin Two-Dimensional Nanomaterials. *ACS Nano* 9 (10), 9451–9469. doi:10.1021/acsnano.5b05040

Zhang, W.-H., Ding, S.-J., Zhang, Q.-S., Yi, H., Liu, Z.-X., Shi, M.-L., et al. (2021). Rare Earth Element-Doped Porous In_2O_3 Nanosheets for Enhanced Gas-Sensing Performance. *Rare Met.* 40 (6), 1662–1668. doi:10.1007/s12598-020-01607-x

Zhang, Y., Zeng, W., and Li, Y. (2019). NO_2 and H_2 Sensing Properties for Urchin-like Hexagonal WO_3 Based on Experimental and First-Principle Investigations. *Ceramics Int.* 45 (5), 6043–6050. doi:10.1016/j.ceramint.2018.12.075

Zheng, H., Ou, J. Z., Strano, M. S., Kaner, R. B., Mitchell, A., and Kalantar-zadeh, K. (2011). Nanostructured Tungsten Oxide - Properties, Synthesis, and Applications. *Adv. Funct. Mater.* 21 (12), 2175–2196. doi:10.1002/adfm.201002477

Conflict of Interest: The authors declare that the research was conducted in the absence of any commercial or financial relationships that could be construed as a potential conflict of interest.

Publisher's Note: All claims expressed in this article are solely those of the authors and do not necessarily represent those of their affiliated organizations, or those of the publisher, the editors, and the reviewers. Any product that may be evaluated in this article, or claim that may be made by its manufacturer, is not guaranteed or endorsed by the publisher.